

A fluorescent heteroditopic ligand responding to free zinc ion over six orders of magnitude concentration range†

Lu Zhang,^a Christopher S. Murphy,^b Gui-Chao Kuang,^a Kristin L. Hazelwood,^b Manuel H. Constantino,^a Michael W. Davidson^{*b} and Lei Zhu^{*a}

Received (in Austin, TX, USA) 9th September 2009, Accepted 16th October 2009

First published as an Advance Article on the web 4th November 2009

DOI: 10.1039/b918729d

A fluorescent heteroditopic ligand useful in live-cell imaging studies responds to free zinc ion concentration over a range of six orders of magnitude in a buffered aqueous solution via dual-channel fluorescence.

The biological functions of zinc ion are multifaceted:^{1,2} it (a) serves as a catalytic cofactor for many metalloenzymes, (b) supports functional tertiary structures of various proteins, and (c) mediates neuronal signal transduction events.³ Consequently, the fluctuation of free (available for protein binding)^{4,5} zinc ion concentration ($[Zn]_f$) may profoundly affect the physiological state of an organism. Three classes of proteins: transporters, sensors, and metallothioneins, work in concert in regulating zinc homeostasis.⁶ Their activities are dependent on the type and developmental stage of cells. Such dependence leads to the varied availability (or concentration) of free zinc across an organism.

The mechanistic details of zinc homeostasis are not entirely clear,^{7,8} partly due to the difficulty in directly mapping the distribution and tracking the movement of the spectroscopically inert free zinc ions. Therefore, zinc ion-selective fluorescent probes have been the primary tools for the detection and quantification of biological free zinc. The past decade has witnessed the rapid progress in the development of zinc probes,^{9–13} which have enabled significant advances in the cell biology of zinc.^{3,11}

Despite the advances, new challenges continue to emerge. For instance, it is known that the concentrations of free zinc range from sub-nanomolar⁵ to almost millimolar¹⁴ depending on cell and organelle types. Quantification over the entire physiological range would require probes whose fluorescent signals do not saturate over a concentration span ranging six orders of magnitude. Some attempts have been made to address this issue, for example, by using a collection of probes with different detection ranges.^{15–18} However, in addition to being labor-intensive because parallel experiments are needed,

the cellular uptake efficiencies of various probes may differ, which complicates quantitative measurements. Individual probes that are capable of zinc quantification over large concentration ranges will be far superior. The demand for such probes is underscored by the unique challenges in zinc neurobiology. For example, presynaptic release of zinc in neurons at high or low concentrations has been postulated to induce the activities of either high-affinity voltage independent (HAVI) or low-affinity voltage dependent (LAVD) zinc receptors at the postsynaptic density (PSD).¹⁹ Therefore, the quantitative information of zinc fluctuation during a brain neuronal event could be best obtained by using a single probe applicable over a broad concentration range. The zinc-release data can be correlated to the expression of HAVI or LAVD receptors which may prove pivotal in unraveling the zinc-involved signal transduction pathways in brain neurobiology.

To design a probe with a broad concentration coverage, we first simulated the fluorescence responses to $[Zn]_f$ of probes containing single zinc-binding sites. The effective concentration range of a “monotopic” probe is ~ 3 orders of magnitude, inadequate for covering the entire concentration range of biological free zinc (Fig. S1†). On the other hand, if the responses from two monotopic probes with an affinity difference of $\sim 10^3$ were combined, an expanded range of 6 orders of magnitude could be achieved. When the signal of the high-affinity probe is close to saturation, the low-affinity probe begins to operate. Therefore, by including two different zinc coordination sites in one molecule and translating the information of species distribution into fluorescence, fluorescent zinc probes with six orders of magnitude concentration coverage are attainable.

Our interest in zinc coordination chemistry and sensing^{20,21} led to a fluorescent heteroditopic ligand platform (Fig. 1) capable of correlating three coordination states (non-, mono-, and di-coordinated) to three fluorescence states (OFF, ON at one color, ON at a different color) in acetonitrile.^{22–25} This structural framework is ideal for developing zinc probes effective over large concentration ranges. The ligand is designed to have a low fluorescence quantum yield (ϕ_f) due to intramolecular photoinduced electron transfer (PET)^{26–28} from Q (the Quencher, also the high-affinity zinc binding group) to the excited F (the Fluorophore). In the presence of zinc, the ion preferentially binds with the high-affinity site Q to result in fluorescence enhancement at λ_1 .²⁶ The intensity at λ_1 can be used to correlate zinc concentration values at the low end. When zinc concentration is high enough to bind with the second, low-affinity site within F, stabilization of the

^a Department of Chemistry and Biochemistry, Florida State University, Tallahassee, FL 32306-4390, USA.
E-mail: lzhu@chem.fsu.edu; Fax: +1 850 644 8281;
Tel: +1 850 645 6813

^b National High Magnetic Field Laboratory and Department of Biological Science, Florida State University, 1800 East Paul Dirac Drive, Tallahassee, FL 32310, USA. E-mail: davidson@magnet.fsu.edu;
Fax: +1 850 644 8920; Tel: +1 850 644 0542

† Electronic supplementary information (ESI) available: Procedures for syntheses, absorption and emission titration studies, and live-cell imaging experiments. Additional spectra, DIC images, and co-localization scatterplots were included. See DOI: 10.1039/b918729d

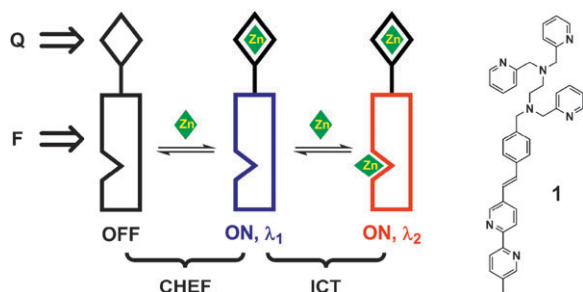


Fig. 1 Left: working principle of a fluorescent heteroditopic ligand. Details in the text. Q: Quencher; F: Fluorophore; CHEF: CHElation-Enhanced Fluorescence; ICT: Internal (or Intramolecular) Charge Transfer. Right: structure of compound **1**.

charge-transfer (CT) excited state upon coordination results in an emission bathochromic shift from λ_1 to λ_2 .²⁹ Therefore, the intensity at λ_2 , or the intensity ratio at λ_2 and λ_1 , can be used to relate zinc concentration at the high end.

Heteroditopic ligand **1** reported herein is shown in Fig. 1. The high-affinity site is the *N,N,N'*-tris(pyridylmethyl)-ethylenediamine group, which has been extensively used for zinc binding.³⁰ Other studies showed that this polyaza moiety is selective for zinc over calcium and magnesium, the two metals that might interfere with fluorescence imaging of cellular zinc, by 8–10 orders of magnitude in affinity.^{30,31} The low-affinity site is the 2,2'-bipyridyl (bipy) site, which is part of the fluorophore. The synthesis of **1** is described in the ESI†. Similar to the reported model system,²² **1** shows fluorescence enhancement followed by an emission bathochromic shift upon zinc addition in acetonitrile (ESI†). The following discussion pertains to studies in aqueous solutions.

Similar to the eukaryotic cellular environments,^{5,32} a zinc ion buffer system was used in the titration experiments where the total zinc ion concentrations were high and the free zinc concentrations were controlled by metal ion chelators EDTA, HEDTA, EGTA, and NTA. The absorption spectrum of **1** undergoes an overall bathochromic shift upon addition of zinc (Fig. S5†) due to the eventual coordination at the bipy site to result in the stabilization of the ICT excited state. Similar to the observations in acetonitrile, the fluorescence undergoes an enhancement prior to a bathochromic shift (Fig. 2A). The sequential coordination at the high- and low-affinity binding sites results in CHEF and stabilization of the ICT excited state, respectively. The fluorescence quantum yields (ϕ_f) of various species are listed in Fig. 2A.

The correlation of fluorescence intensity of **1** to $[Zn]_f$ at two wavelengths, which represent the short and long emission bands, reveals the concentration range of free zinc that **1** can cover for quantitative analysis (Fig. 2B). The fluorescence intensity at the short wavelength channel (409 nm) is sensitive to the change of $[Zn]_f$ from 10^{-14} M to 10^{-11} M; whereas the intensity at the long wavelength channel (480 nm) can be related to $[Zn]_f$ from 10^{-11} M to 10^{-8} M. As suggested by Fig. S1,† by combining the coverage of both channels, the overall $[Zn]_f$ coverage of **1** spans from 10^{-14} M to 10^{-8} M, a range of six orders of magnitude.

The applicability of **1** in live-cell imaging was evaluated. HeLa cells (CCL2 line) absorb **1** readily upon incubation up to

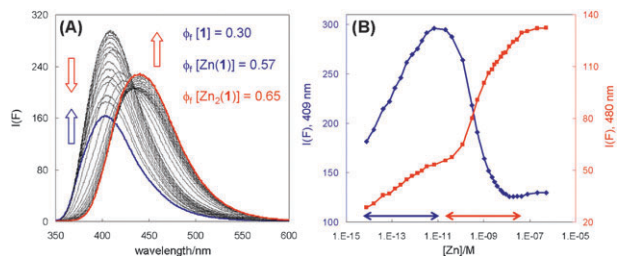


Fig. 2 Fluorescence (A, $\lambda_{\text{ex}} = 340$ nm) of **1** (2 μM) at various free zinc concentrations ($[Zn]_f$) in 10% DMSO aqueous solution (HEPES: 50 mM, pH = 7.0, KNO_3 : 100 mM; EDTA: 5 mM; HEDTA: 5 mM; EGTA: 5 mM; NTA: 5 mM). The blue and red arrows represent spectral changes when $[Zn]_f$ is low and high, respectively. The ϕ_f values of three coordination states are listed. (B) The fluorescence intensity at 409 nm and 480 nm, respectively. The double-headed arrows represent the concentration ranges covered by the two wavelength channels.

30 min. Weak fluorescence was observed without addition of zinc using the Q-Max Blue filter set (Omega Optical). The background fluorescence (Fig. 3B) was primarily a result from the zinc content in the culture media. It was mostly eliminated after the addition of the membrane-permeable, high-affinity zinc chelator TPEN (Fig. 3A). Upon increasing zinc concentration up to 100 μM , the fluorescence intensity rises as observed in the window of 420 nm to 480 nm (Fig. 3). The overall fluorescence enhancement at this particular excitation/emission profile was anticipated based on the solution absorption and emission titration studies (Fig. 2 and S5†). **1** and its zinc complex do not appear toxic during the experiment based on the lack of change in cell morphology.

The subcellular localization properties of **1** were studied by co-staining experiments using organelle-specific probes. **1** and its zinc complex localize in mitochondria as indicated by high Pearson's coefficients (PC, 0.86 and 0.90, respectively, Fig. 4D) determined by co-localization scatterplots (Fig. S7†).³³ Mitochondrial zinc can be used for assembling zinc metallo-enzymes. However, the complete functional profile of the mitochondrial zinc remains largely uncharacterized.³⁴

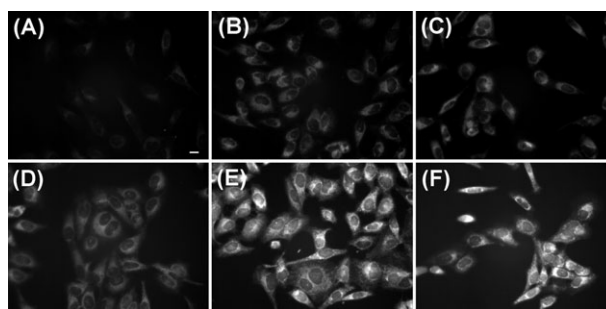


Fig. 3 (A) to (F): fluorescence images of live HeLa cells (37 °C, 5% CO_2) with added $[\text{ZnCl}_2]$ at 0 (with 20 μM TPEN), 0, 5 μM , 10 μM , 50 μM , and 100 μM , respectively (DIC images in ESI†). The cells were incubated with **1** (10 μM) and MitoTracker Red (0.3 μM) for 30 min before media was replaced. The cells were then incubated with ZnCl_2 /pyrithione solutions ($[\text{ZnCl}_2]$ from 0 to 100 μM ; [pyrithione] = 20 μM) for 10 min. The fluorescence images were acquired using a Q-Imaging Retiga camera and an Omega Q-Max Blue filter set (excitation 355–405 nm; emission 420–480 nm) with 500 ms exposure time. The focus was adjusted in the red channel (MitoTracker Red). Scale bar: 10 μm .

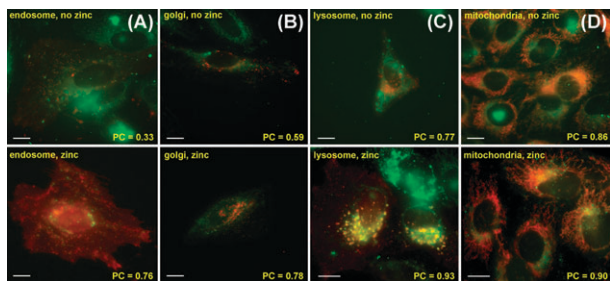


Fig. 4 Green channel: **1** (top), $[\text{Zn}(\mathbf{1})]^{2+}$ (bottom). Red channel: (A) Fusion of mApple fluorescent protein with an endosomal targeting peptide. (B) mApple fused to a Golgi targeting peptide. (C) mApple fused to lysosomal membrane glycoprotein 1 (LAMP1). (D) MitoTracker Red CMXRos. Scale bar: 10 μm .

The physiological significance of mitochondrial zinc has been investigated using zinc-selective fluorescent probes.³⁵ Evidence suggests that mitochondria function as independently operated endogenous zinc pools which are both sources and sinks during zinc homeostasis.³⁵ The availability of mitochondria-targeting zinc probes with broad concentration coverages is expected to facilitate the investigations of zinc transport between several intracellular zinc pools (e.g. mitochondrial, vesicular, and ligand/protein bound).

The localization efficiencies of **1** in other organelles were studied *via* co-staining experiments using organelle-specific fusions to the red fluorescent protein, mApple.³⁶ Compound **1** extensively localizes in Golgi complexes and lysosomes as indicated by Pearson's coefficients over 0.50. **1** does not accumulate in endosomes efficiently (PC = 0.33), suggesting that it might have entered the cell *via* passive permeation through the cell membrane rather than endocytosis. With addition of 100 μM ZnCl_2 , the localization properties of **1** vary. In particular, a very high Pearson's coefficient for lysosomes (0.93) was recorded. The increase of localization of **1** in lysosomes at cytotoxic zinc levels suggests that cells have transported surplus zinc ions to lysosomes for disposal.

In summary, we have demonstrated that through rational design fluorescent heteroditopic ligands for zinc ions can be prepared whose dual-channel fluorescence is capable of correlating $[\text{Zn}]_f$ under simulated physiological conditions over a range of 6 orders of magnitude. The preliminary live-cell imaging studies showed that compound **1** (a) is able to penetrate the cell membrane readily, (b) is not overly toxic to HeLa cells during the course of the experiment, (c) accumulates in mitochondria and to lesser extents in other organelles, and (d) undergoes fluorescence enhancement with increasing zinc gradient. Based on our understanding of the coordination-driven photophysical processes in this heteroditopic platform, we are currently preparing variants of compound **1** with lower excitation energies to reduce the likelihood of autofluorescence from cellular samples, and larger spectral separations of two wavelength channels so that the intensity at each channel can be collected using matching filter sets in live-cell imaging experiments.

This work was supported by FSU through a start-up fund, a New Investigator Research (NIR) grant (08KN-16) from the James & Esther King Biomedical Research Program administered by FL DOH, and NSF (CHE 0809201).

Notes and references

- B. L. Vallee and K. H. Falchuk, *Physiol. Rev.*, 1993, **73**, 79.
- J. M. Berg and Y. Shi, *Science*, 1996, **271**, 1081.
- C. J. Frederickson, J.-Y. Koh and A. I. Bush, *Nat. Rev. Neurosci.*, 2005, **6**, 449.
- L. A. Finney and T. V. O'Halloran, *Science*, 2003, **300**, 931.
- A. Krezel and W. Maret, *JBIC, J. Biol. Inorg. Chem.*, 2006, **11**, 1049.
- W. Maret, *BioMetals*, 2001, **14**, 187.
- D. H. Nies, *Science*, 2007, **317**, 1695.
- A. Krezel, Q. Hao and W. Maret, *Arch. Biochem. Biophys.*, 2007, **463**, 188.
- K. Kikuchi, H. Komatsu and T. Nagano, *Curr. Opin. Chem. Biol.*, 2004, **8**, 182.
- R. B. Thompson, *Curr. Opin. Chem. Biol.*, 2005, **9**, 526.
- C. J. Chang and S. J. Lippard, *Met. Ions Life Sci.*, 2006, **1**, 61.
- Z. Dai and J. W. Canary, *New J. Chem.*, 2007, **31**, 1708.
- E. M. Nolan and S. J. Lippard, *Acc. Chem. Res.*, 2009, **42**, 193.
- S. Y. Assaf and S.-H. Chung, *Nature*, 1984, **308**, 734.
- K. Komatsu, K. Kikuchi, H. Kojima, Y. Urano and T. Nagano, *J. Am. Chem. Soc.*, 2005, **127**, 10197.
- E. M. Nolan, J. Jaworski, K.-I. Okamoto, Y. Hayashi, M. Sheng and S. J. Lippard, *J. Am. Chem. Soc.*, 2005, **127**, 16812.
- M. D. Shultz, D. A. Pearce and B. Imperiali, *J. Am. Chem. Soc.*, 2003, **125**, 10591.
- C. R. Goldsmith and S. J. Lippard, *Inorg. Chem.*, 2006, **45**, 555.
- P. Paoletti, A. M. Vergnano, B. Barbour and M. Casado, *Neuroscience*, 2009, **158**, 126.
- L. Zhang, S. Dong and L. Zhu, *Chem. Commun.*, 2007, 1891.
- S. Huang, R. J. Clark and L. Zhu, *Org. Lett.*, 2007, **9**, 4999.
- L. Zhang, R. J. Clark and L. Zhu, *Chem.-Eur. J.*, 2008, **14**, 2894.
- L. Zhang, W. A. Whitfield and L. Zhu, *Chem. Commun.*, 2008, 1880.
- L. Zhang and L. Zhu, *J. Org. Chem.*, 2008, **73**, 8321.
- L. Zhu, L. Zhang and A. H. Younes, *Supramol. Chem.*, 2009, **21**, 268.
- A. P. de Silva, H. Q. N. Gunaratne, T. Gunnlaugsson, A. J. M. Huxley, C. P. McCoy, J. T. Rademacher and T. E. Rice, *Chem. Rev.*, 1997, **97**, 1515.
- J. Cody, S. Mandal, L. Yang and C. J. Fahrni, *J. Am. Chem. Soc.*, 2008, **130**, 13023.
- R. Parkesh, T. C. Lee and T. Gunnlaugsson, *Org. Biomol. Chem.*, 2007, **5**, 310.
- B. Valeur and I. Leray, *Coord. Chem. Rev.*, 2000, **205**, 3.
- E. Kawabata, K. Kikuchi, Y. Urano, H. Kojima, A. Odani and T. Nagano, *J. Am. Chem. Soc.*, 2005, **127**, 818.
- Ca^{2+} and Mg^{2+} show little effect on the fluorescence of **1**, which ensures the utility of **1** in intracellular imaging. In general, first-row transition metal ions have high affinities to polyaza ligands such as **1**, most of which (e.g. Cu^{2+}) quenches fluorescence. Cd^{2+} which belongs to the same group with Zn^{2+} elicits similar fluorescence response from **1** (Fig. S8[†]). Despite the coordination promiscuity of polyaza ligands, they are frequently incorporated in intracellular fluorescent indicators because of the trace nature of the interfering ions in a cellular environment.
- R. A. Bozym, R. B. Thompson, A. K. Stoddard and C. A. Fierke, *ACS Chem. Biol.*, 2006, **1**, 103.
- A. Smallcombe, *BioTechniques*, 2001, **30**, 1240.
- F. Pierrel, P. A. Cobine and D. R. Winge, *BioMetals*, 2007, **20**, 675.
- S. Sensi, D. Ton-That, P. G. Sullivan, E. A. Jonas, K. R. Gee, L. K. Kaczmarek and J. H. Weiss, *Proc. Natl. Acad. Sci. U. S. A.*, 2003, **100**, 6157.
- N. C. Shaner, M. Z. Lin, M. R. McKeown, P. A. Steinbach, K. L. Hazelwood, M. W. Davidson and R. Y. Tsien, *Nat. Methods*, 2008, **5**, 545.